Supplementary Information for:

Future changes in seasonal climate predictability

Dillon J. Amaya[1], Nicola Maher, Clara Deser, Michael G. Jacox[1,2], Matthew Newman, Michael A. Alexander[1], Juliana Dias, and Jiale Lou

[1]Physical Science Laboratory, Earth System Research Laboratory, National Oceanic and Atmospheric Administration, 325 Broadway, Boulder, CO 80305, United States

[2]Environmental Research Division, Southwest Fisheries Science Center, National Oceanic and Atmospheric Administration, 99 Pacific St #255A, Monterey, CA 93940, United States

[3]Cooperative Institute for Research in Environmental Sciences, University of Colorado Boulder, 216 UCB, University of Colorado Boulder campus, Boulder, CO 80309, United States

[4]National Center for Atmospheric Research, 1850 Table Mesa Dr, Boulder, CO 80305, United States

Corresponding author: Dillon J. Amaya, dillon.amaya@noaa.gov, 816-916-8348

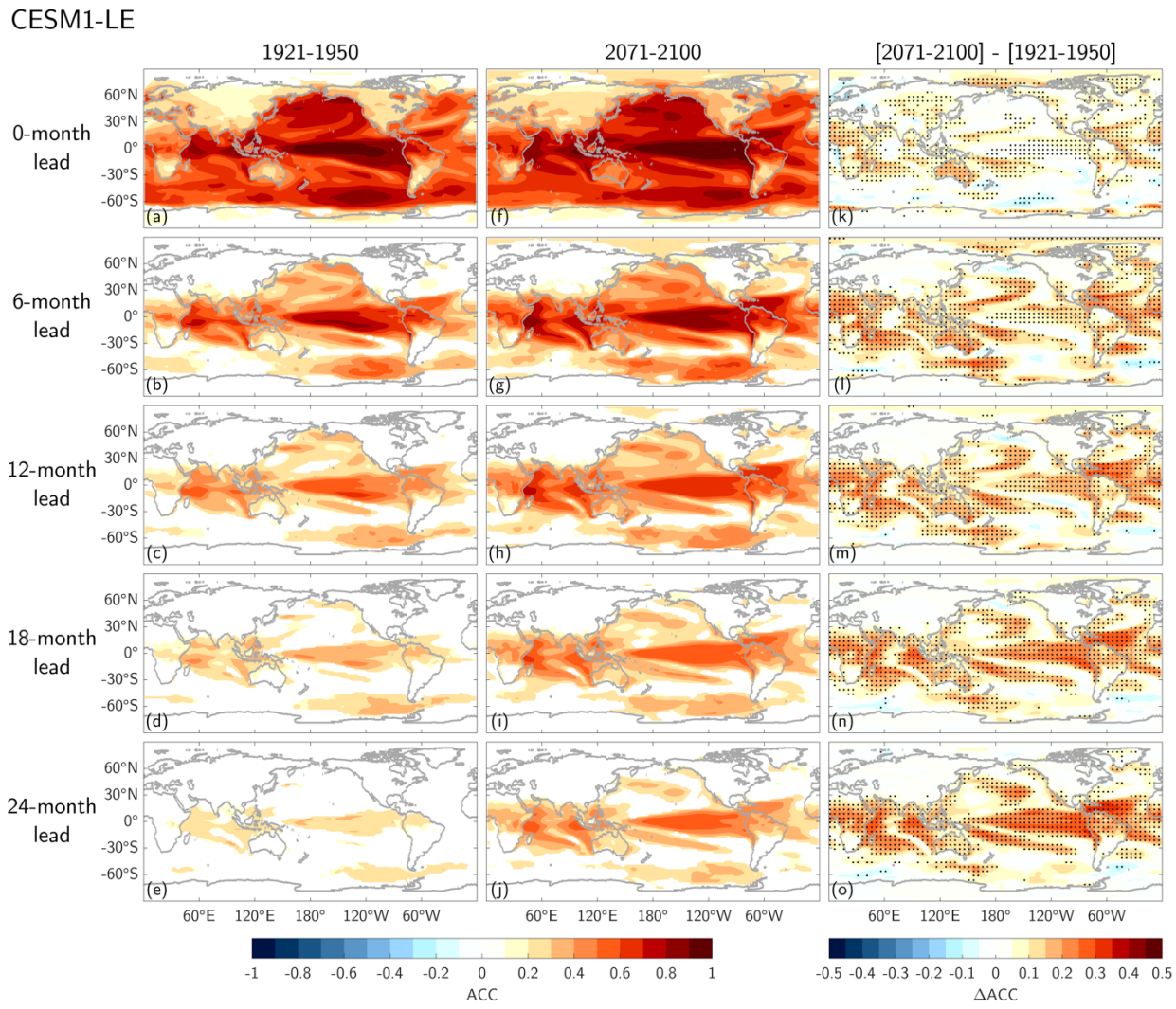

Figure S1 (a)-(e) Ensemble mean potential forecast skill of surface temperature anomalies in CESM1-LE as measured by ACC calculated across all months in the period 1921-1950. (f)-(j) As in (a)-(e), but for the period 2071-2100. (k)-(o) Change in ACC between past and future periods. Skill values in (a)-(j) are only shown when 95% significant. Stipples in (k)-(o) indicate where 80% of a the CESM1-LE ensemble agrees on the sign of the change.

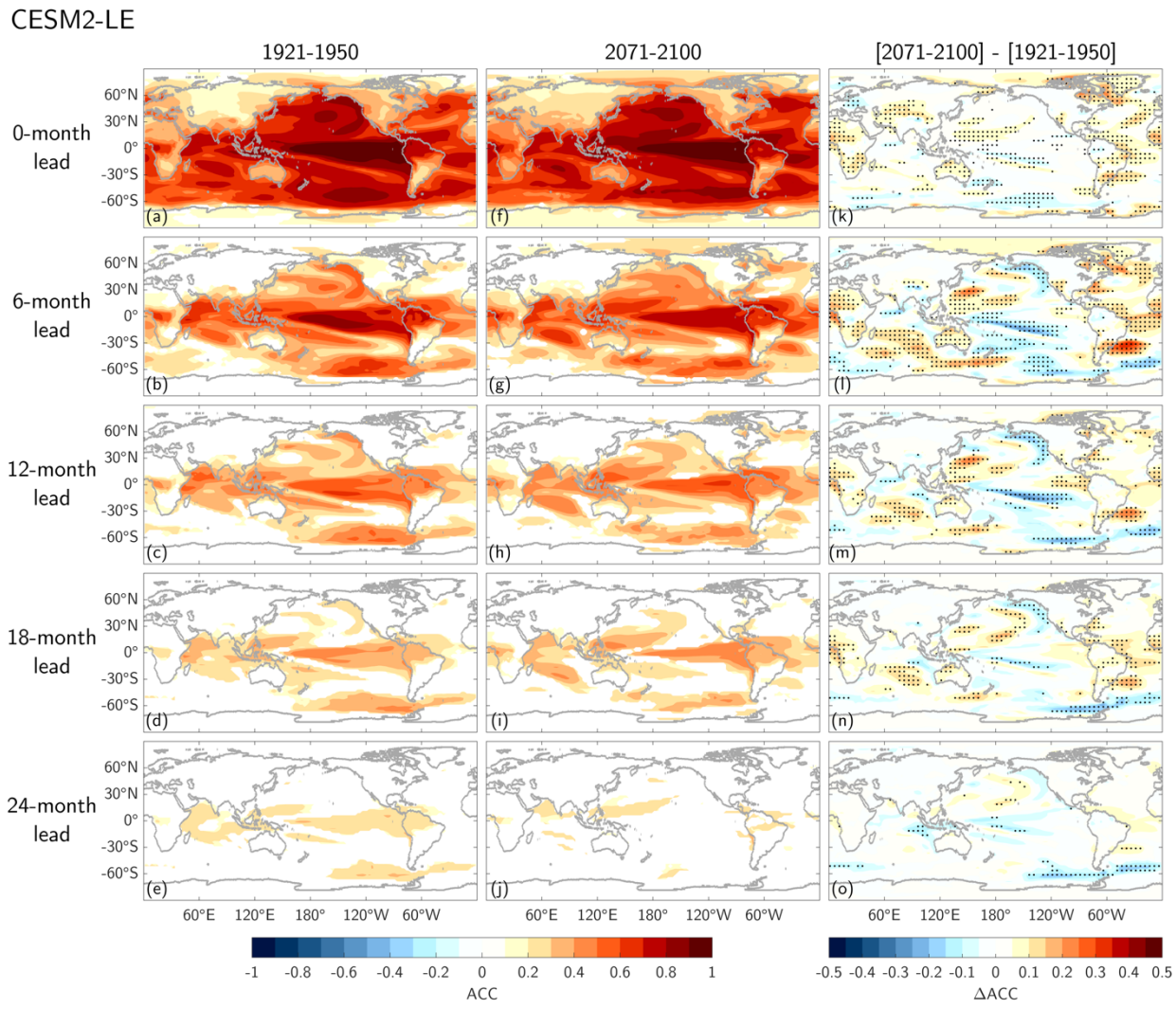

Figure S2 As in Figure S1, but for CESM2-LE.

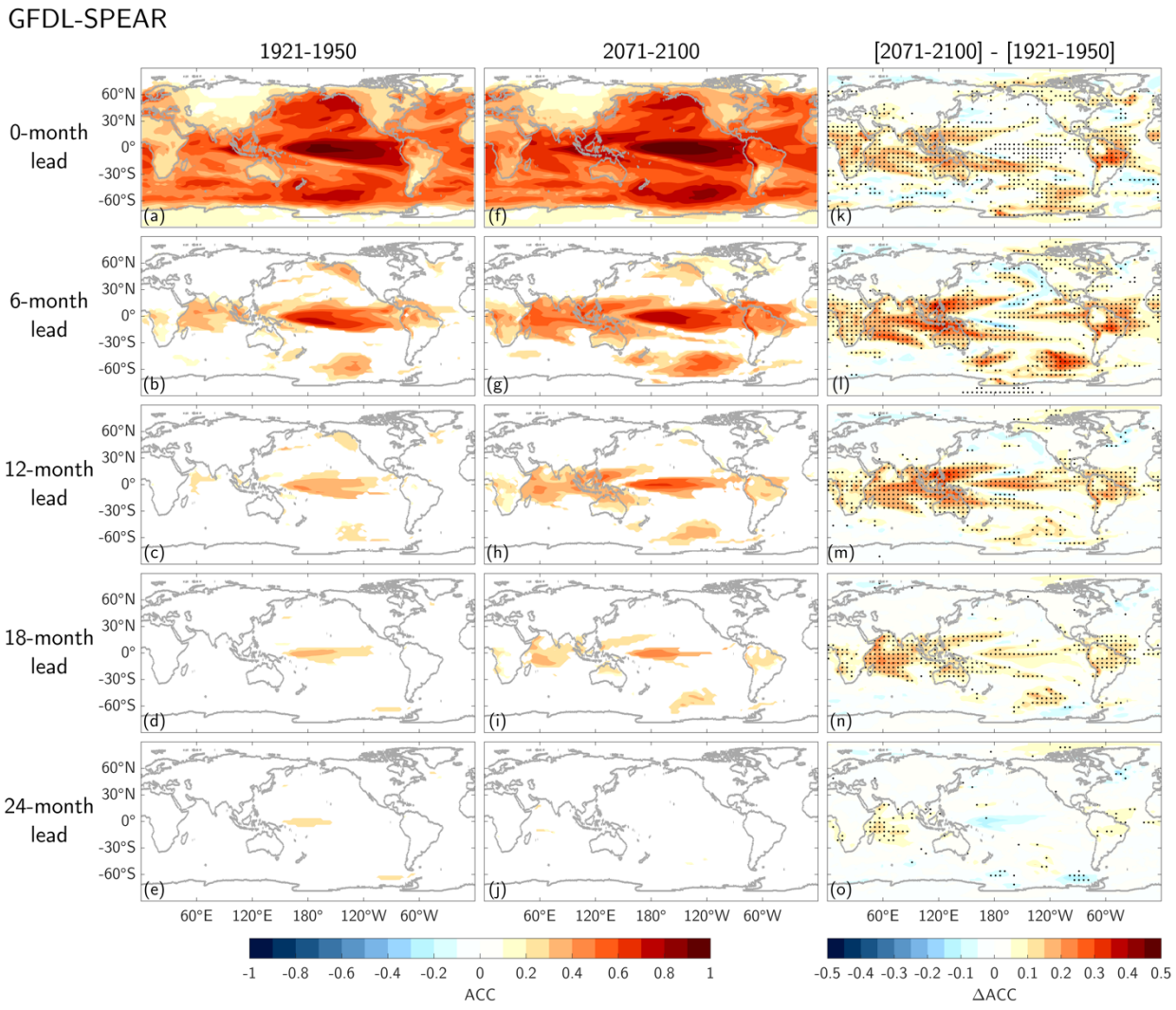

Figure S3 As in Figure S1, but for GFDL-SPEAR.

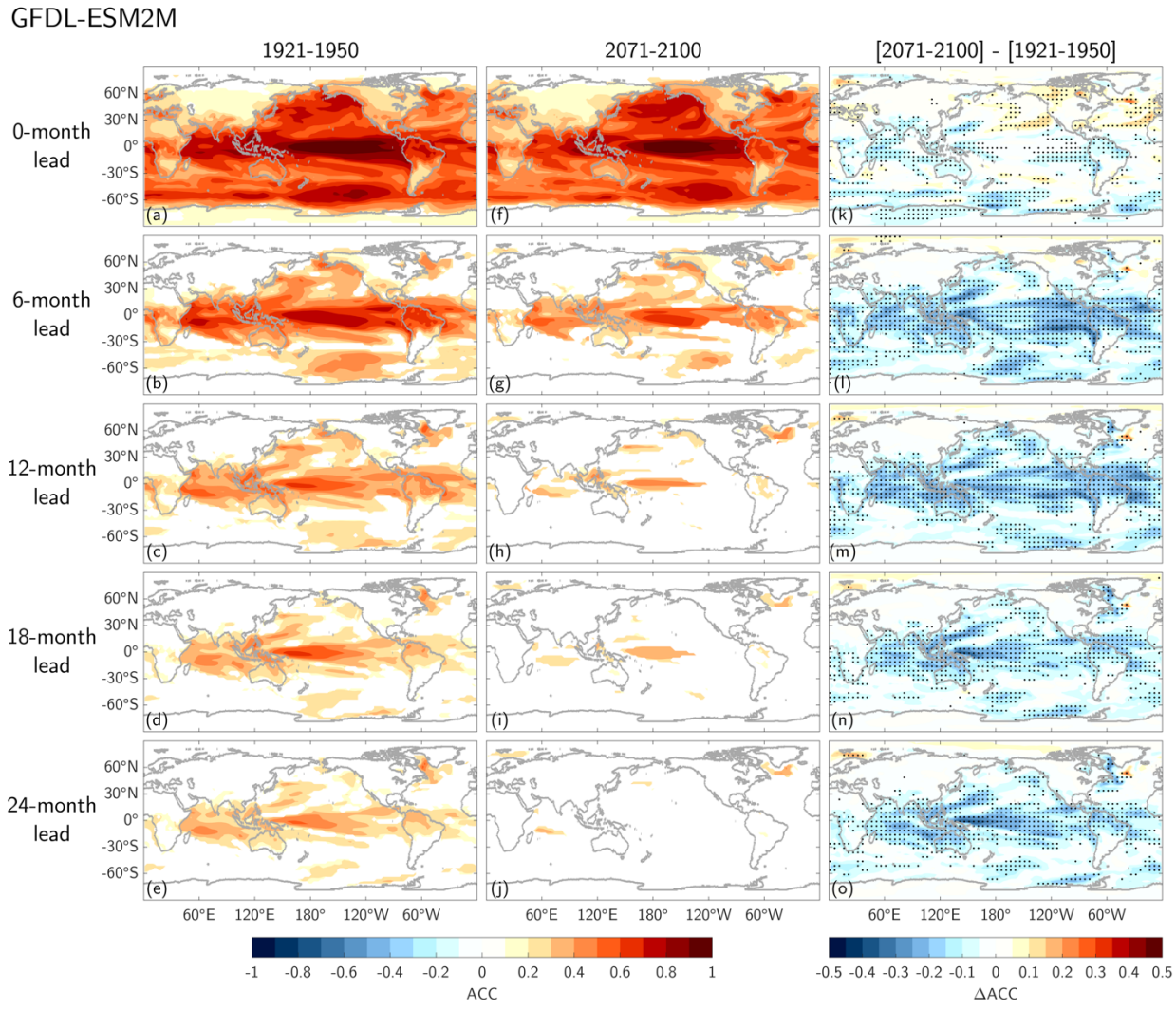

Figure S4 As in Figure S1, but for GFDL-ESM2M.

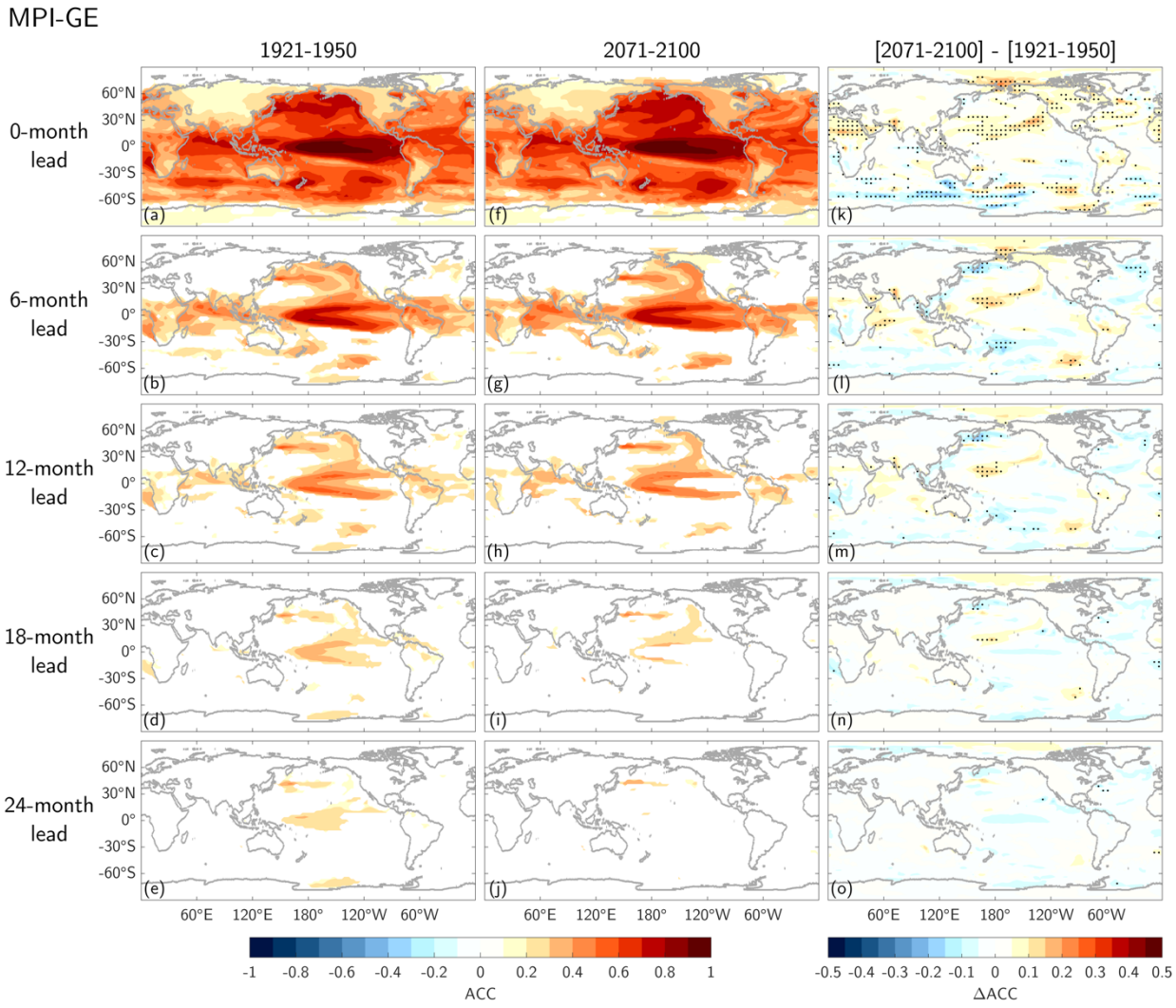

Figure S5 As in Figure S1, but for MPI-GE.

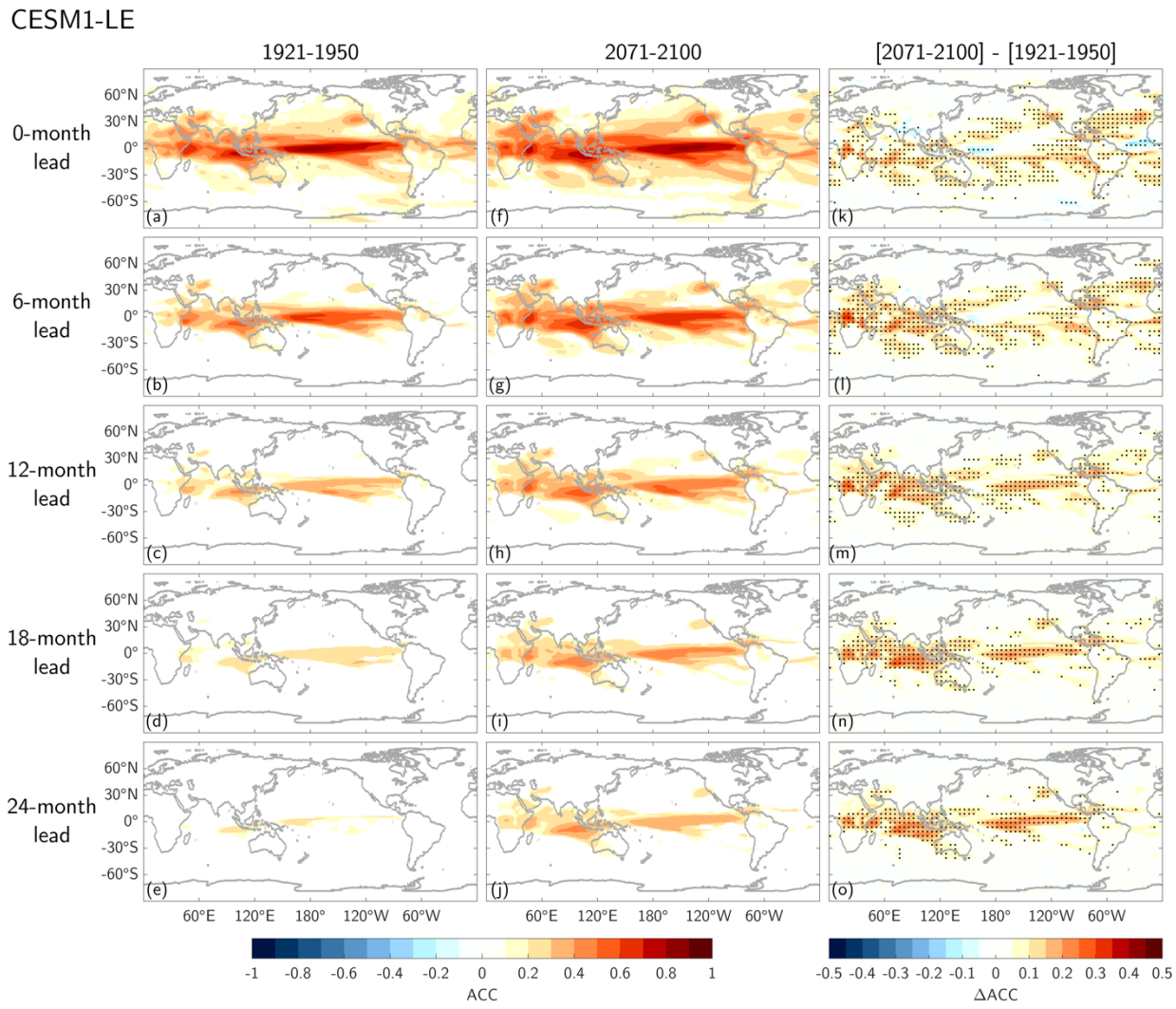

Figure S6 (a)-(e) Ensemble mean potential forecast skill of precipitation anomalies in CESM1-LE as measured by ACC calculated across all months in the period 1921-1950. (f)-(j) As in (a)-(e), but for the period 2071-2100. (k)-(o) Change in ACC between past and future periods. Skill values in (a)-(j) are only shown when 95% significant. Stipples in (k)-(o) indicate where 80% of a the CESM1-LE ensemble agrees on the sign of the change.

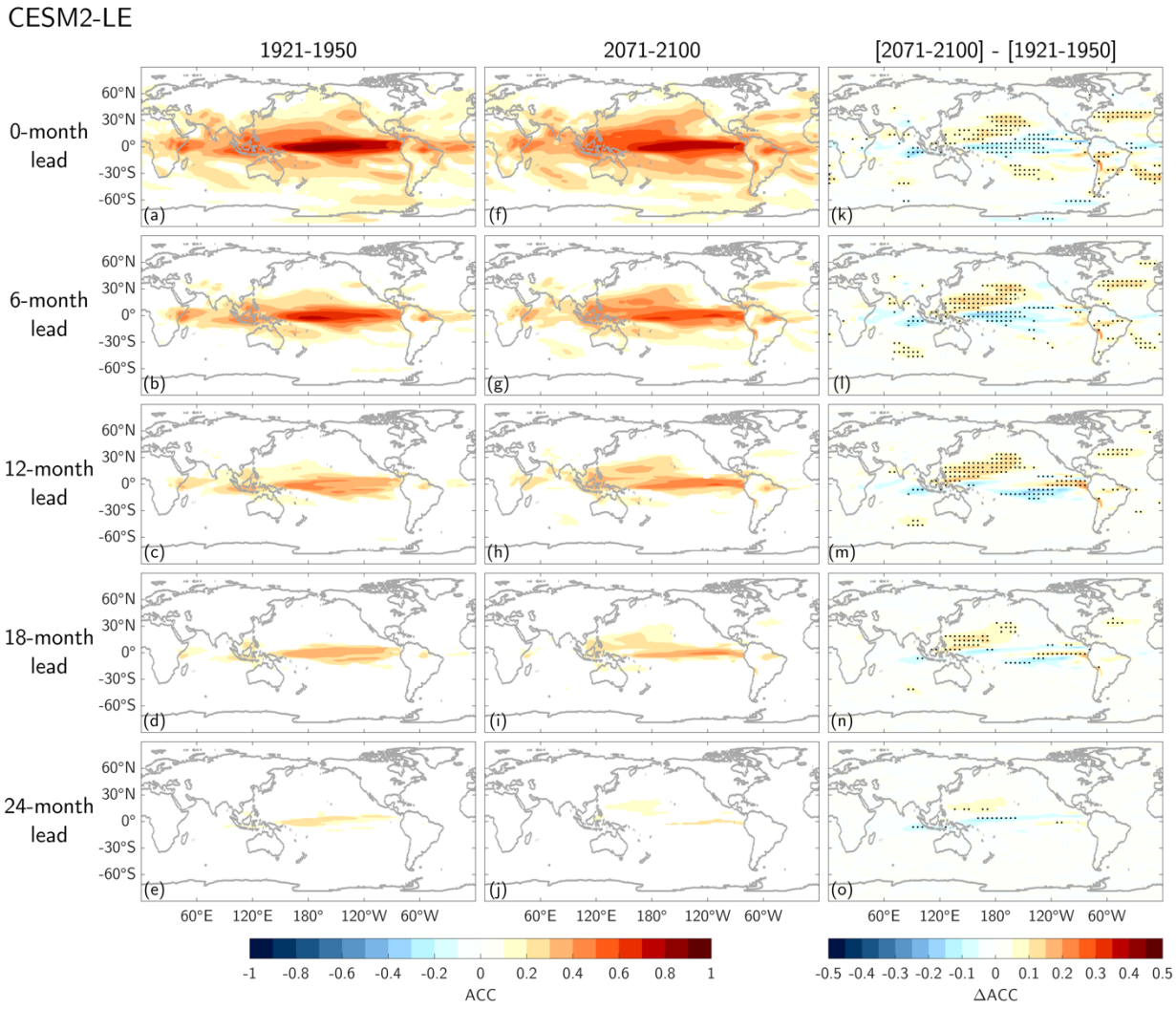

Figure S7 As in Figure S6, but for CESM2-LE.

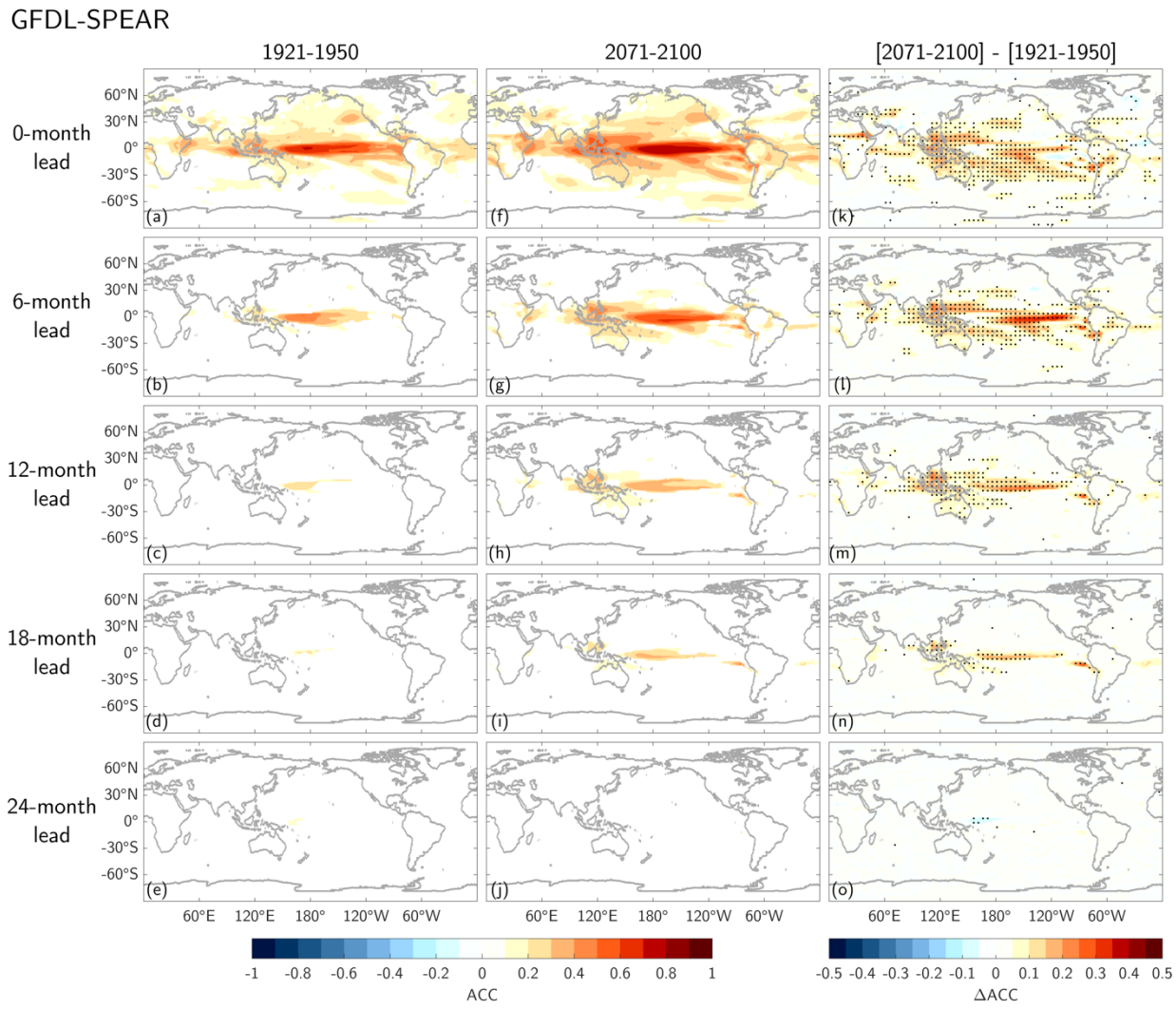

Figure S8 As in Figure S6, but for GFDL-SPEAR.

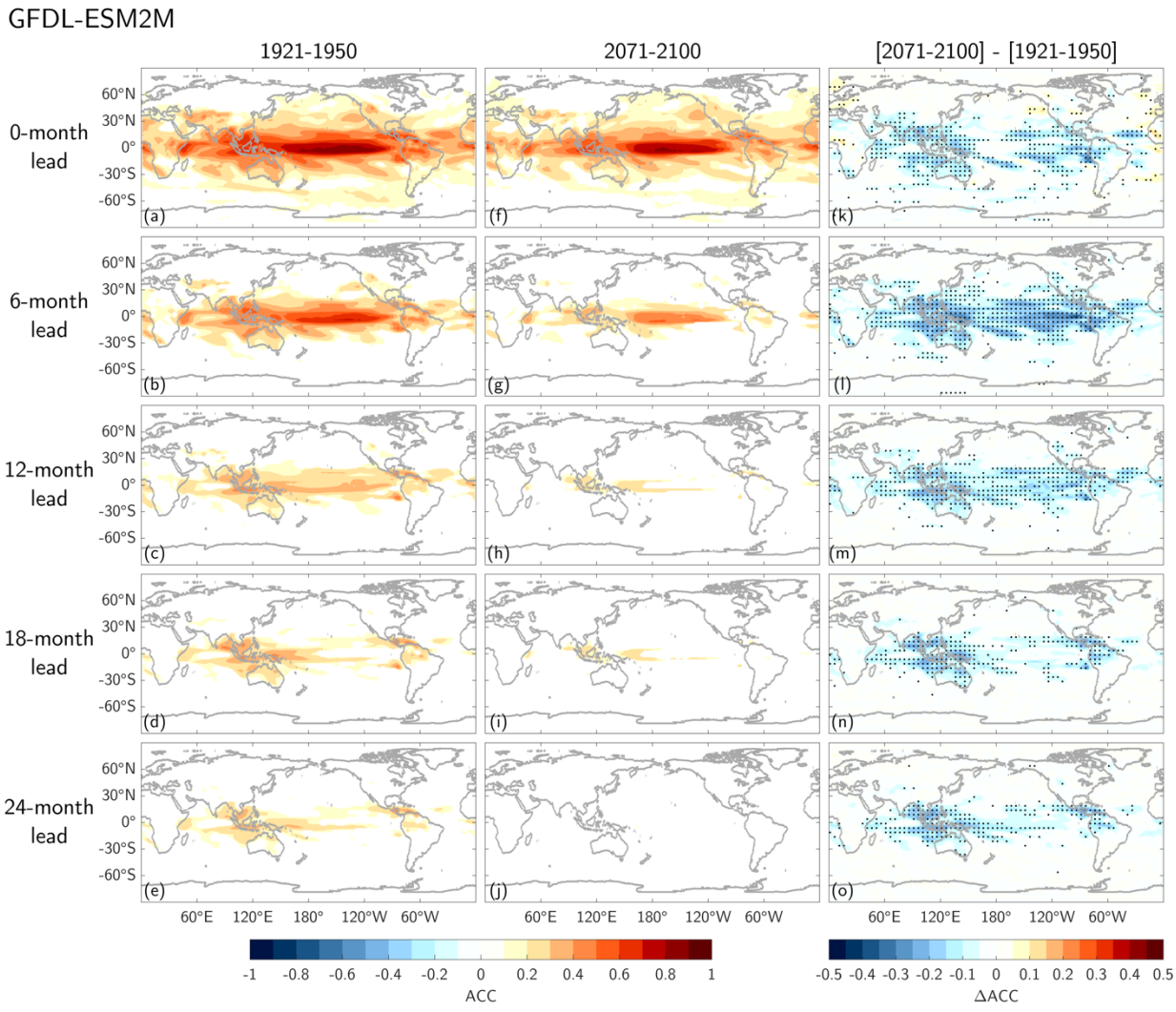

Figure S9 As in Figure S6, but for GFDL-ESM2M.

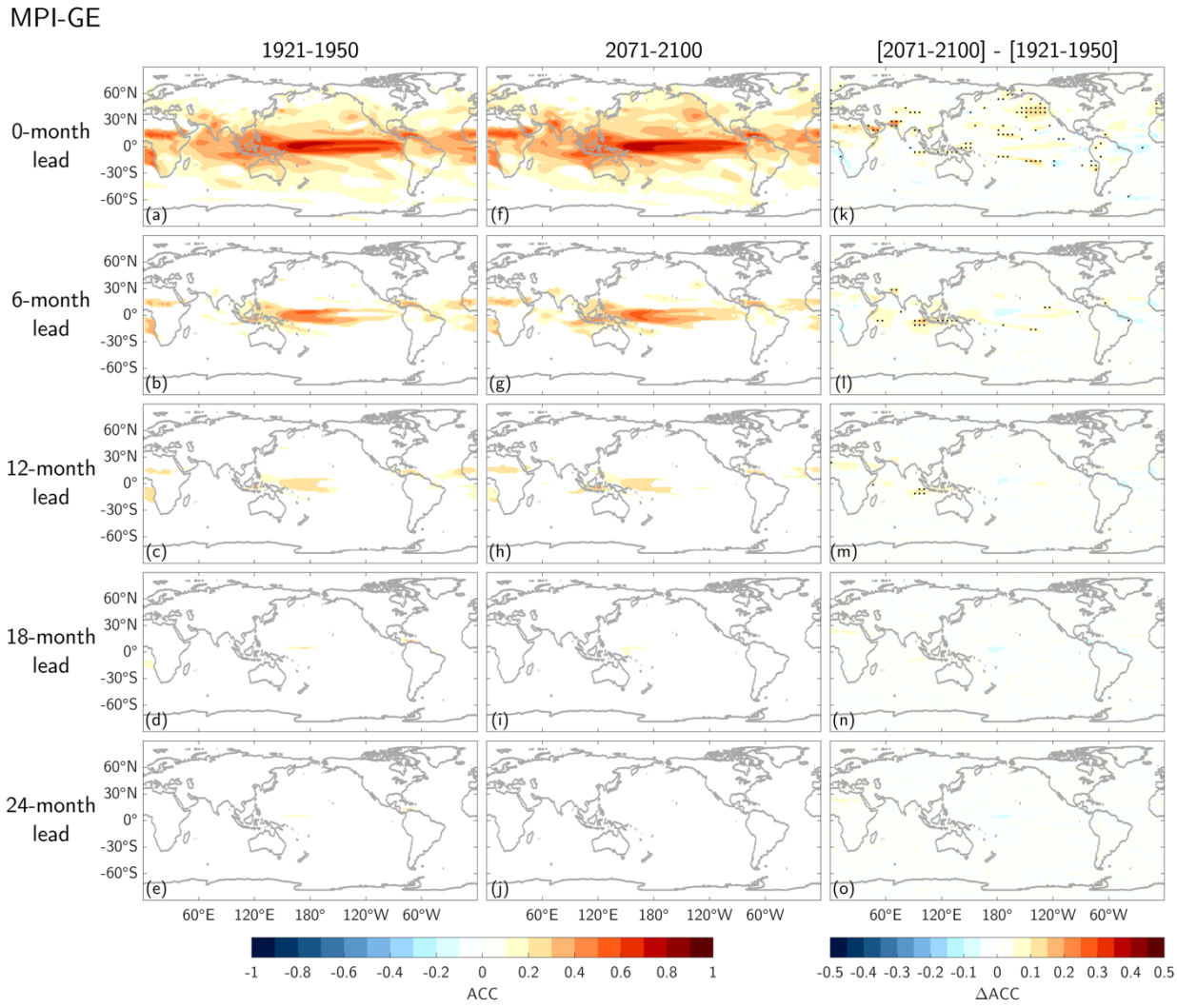

Figure S10 As in Figure S6, but for MPI-GE.

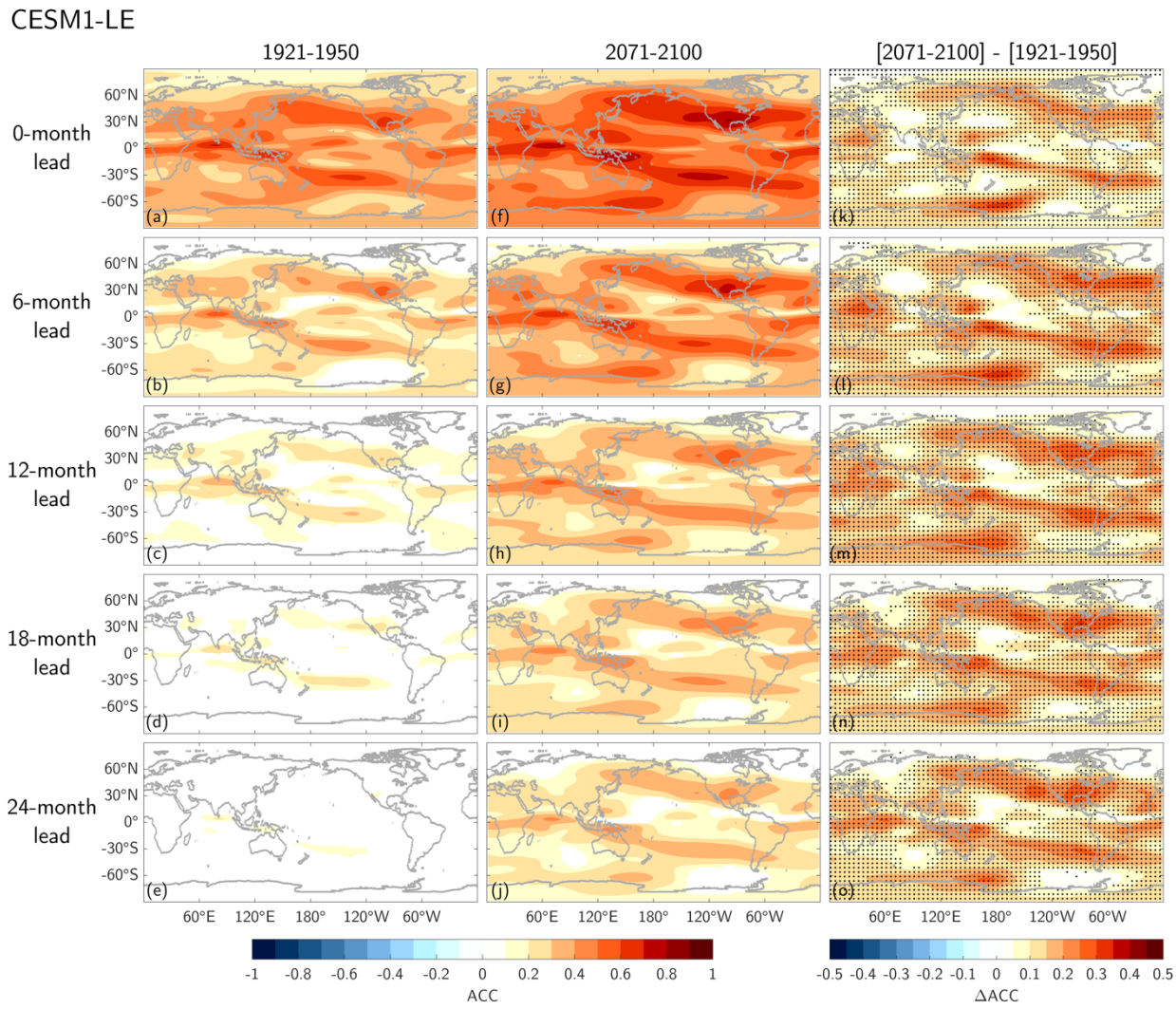

Figure S11 (a)-(e) Ensemble mean potential forecast skill of 500mb streamfunction (ψ_{500}) anomalies in CESM1-LE as measured by ACC calculated across all months in the period 1921-1950. (f)-(j) As in (a)-(e), but for the period 2071-2100. (k)-(o) Change in ACC between past and future periods. Skill values in (a)-(j) are only shown when 95% significant. Stipples in (k)-(o) indicate where 80% of a the CESM1-LE ensemble agrees on the sign of the change.

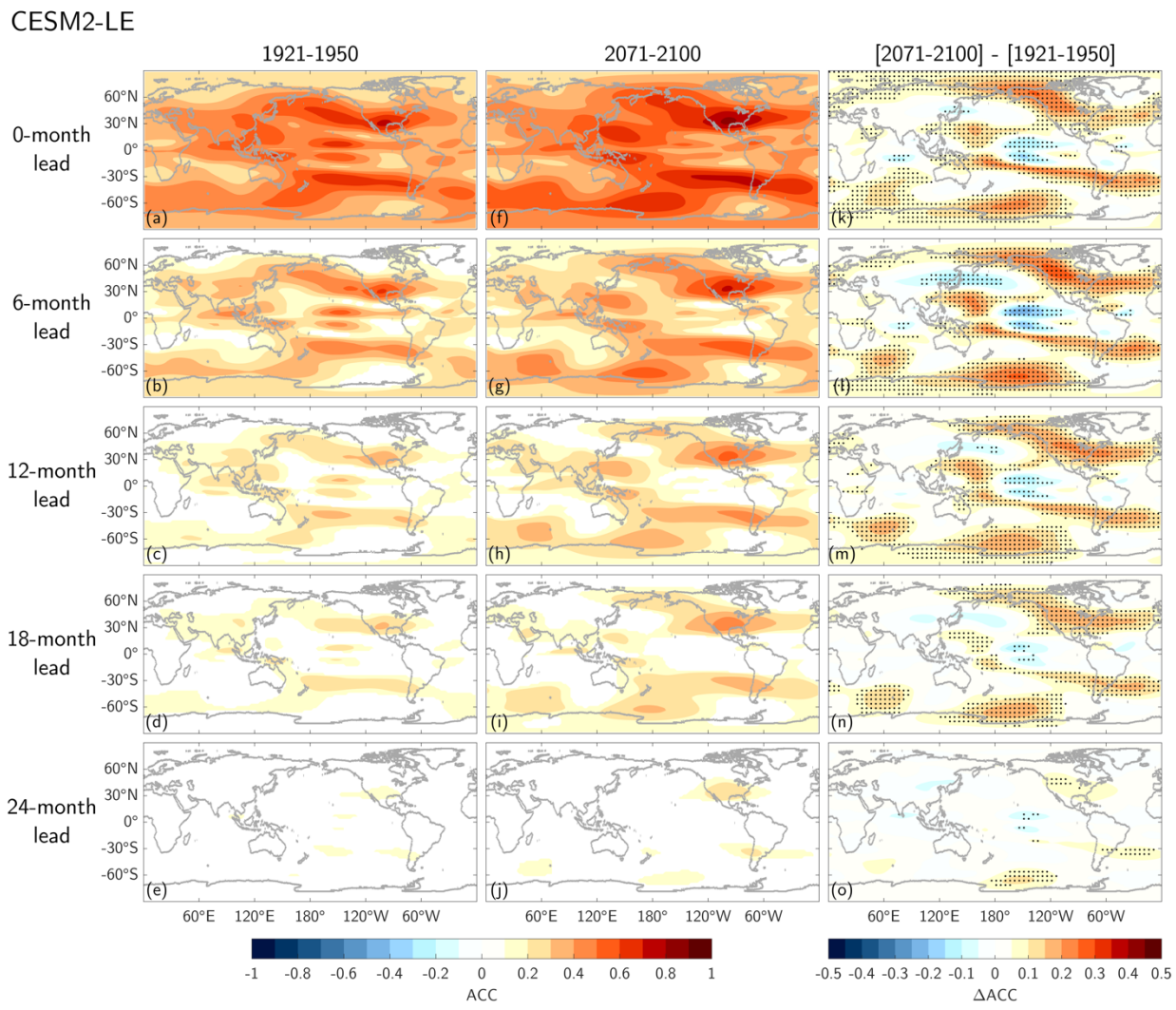

Figure S12 As in Figure S11, but for CESM2-LE.

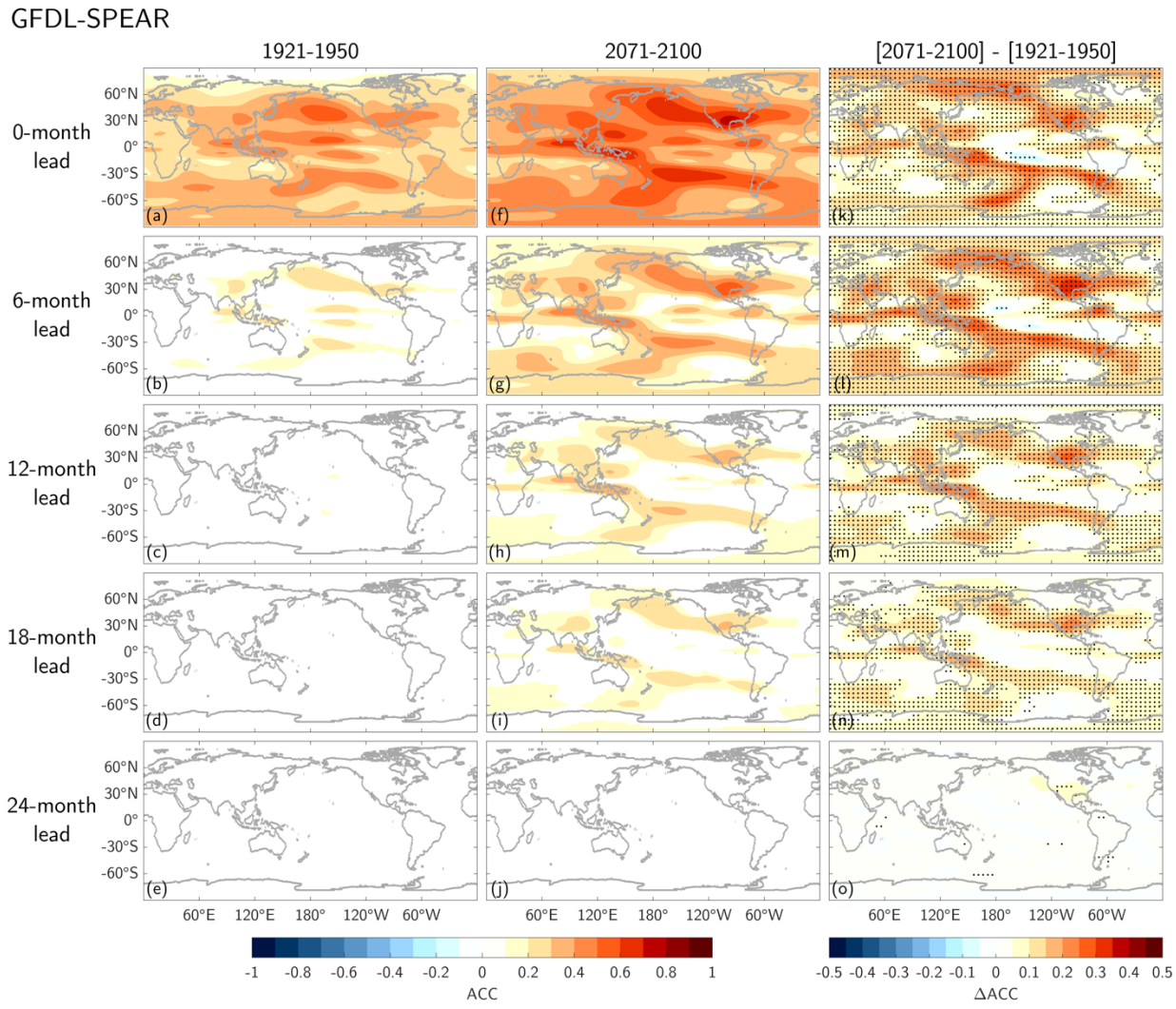

Figure S13 As in Figure S11, but for GFDL-SPEAR.

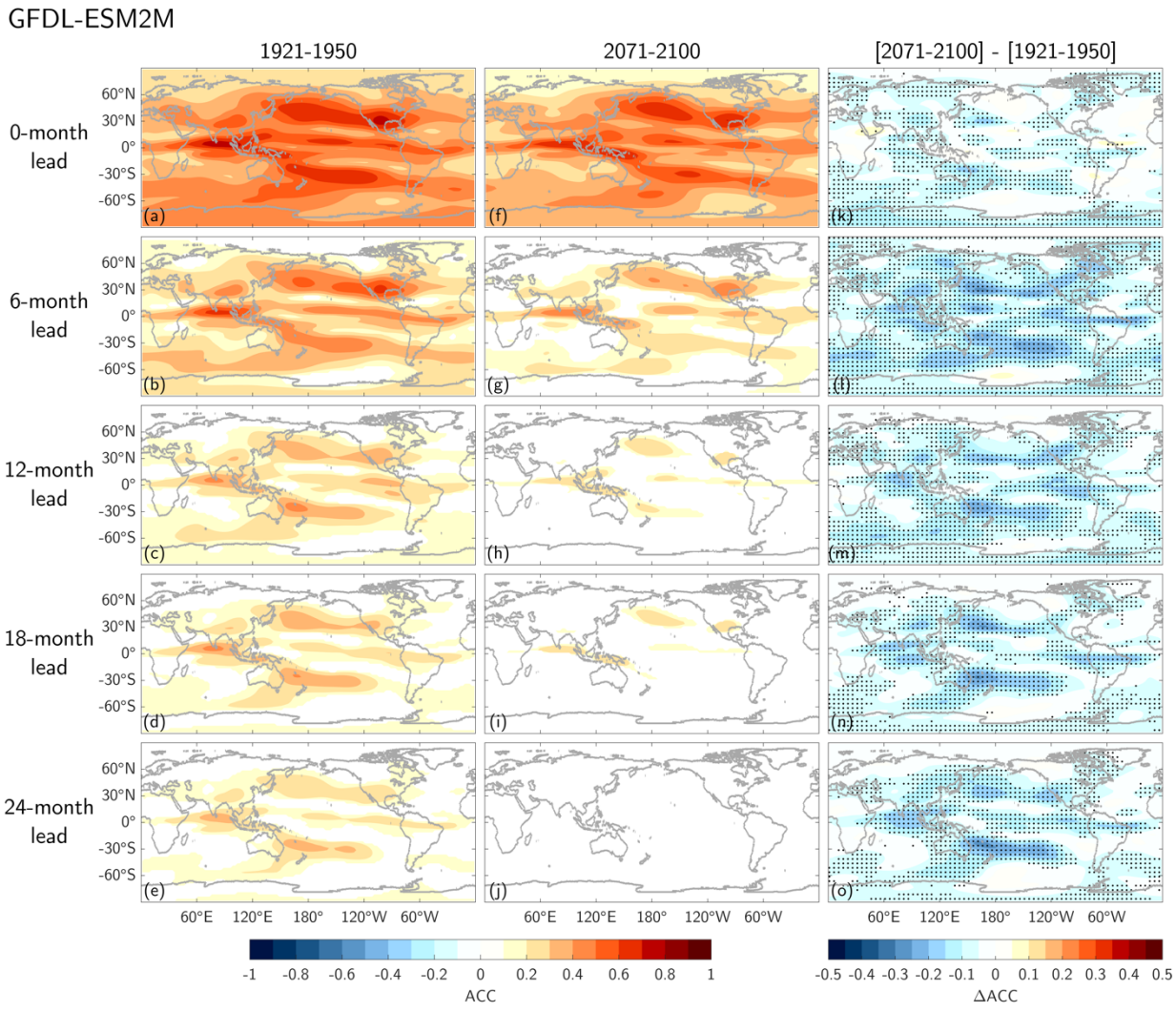

Figure S14 As in Figure S11, but for GFDL-ESM2M.

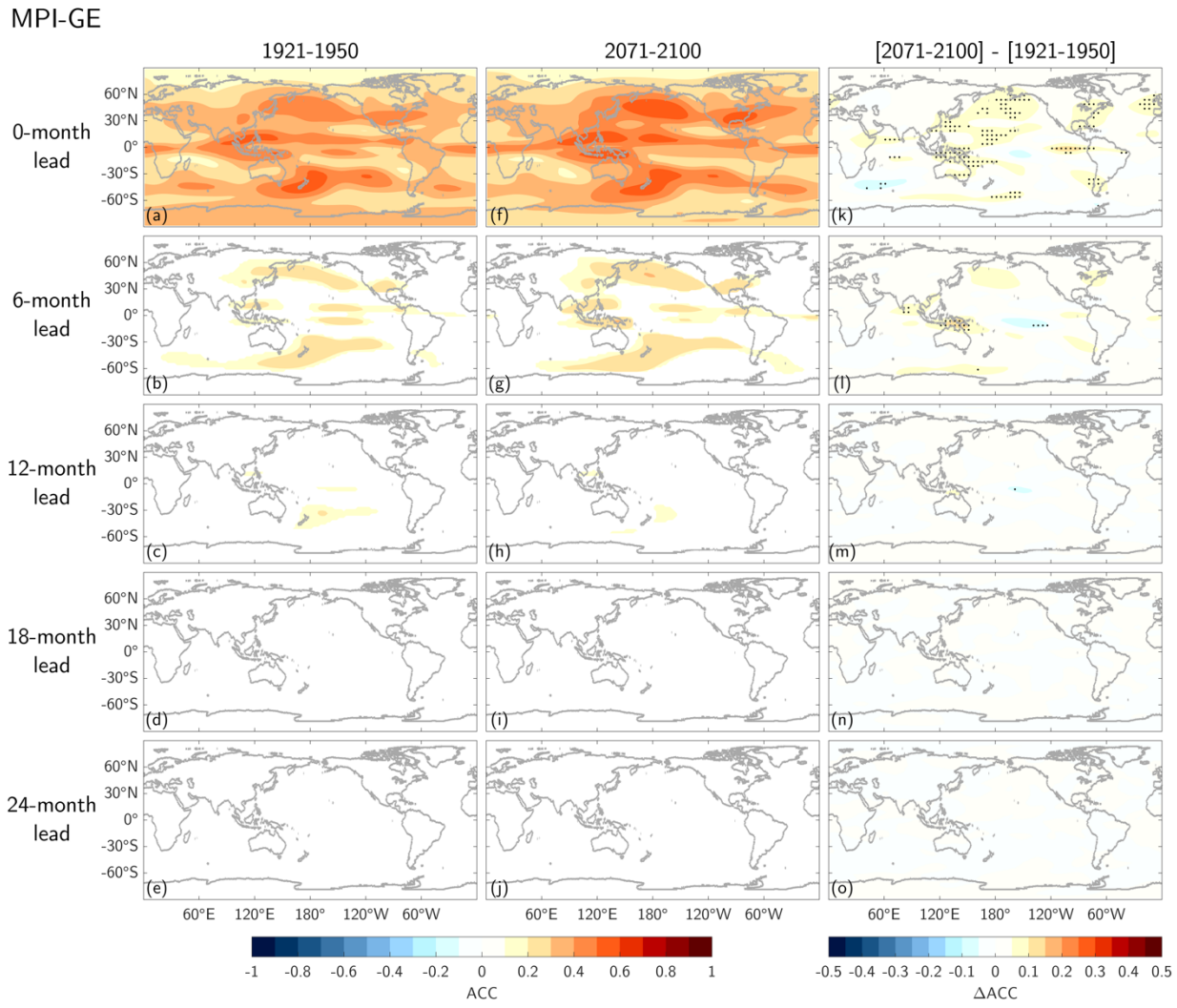

Figure S15 As in Figure S11, but for MPI-GE.

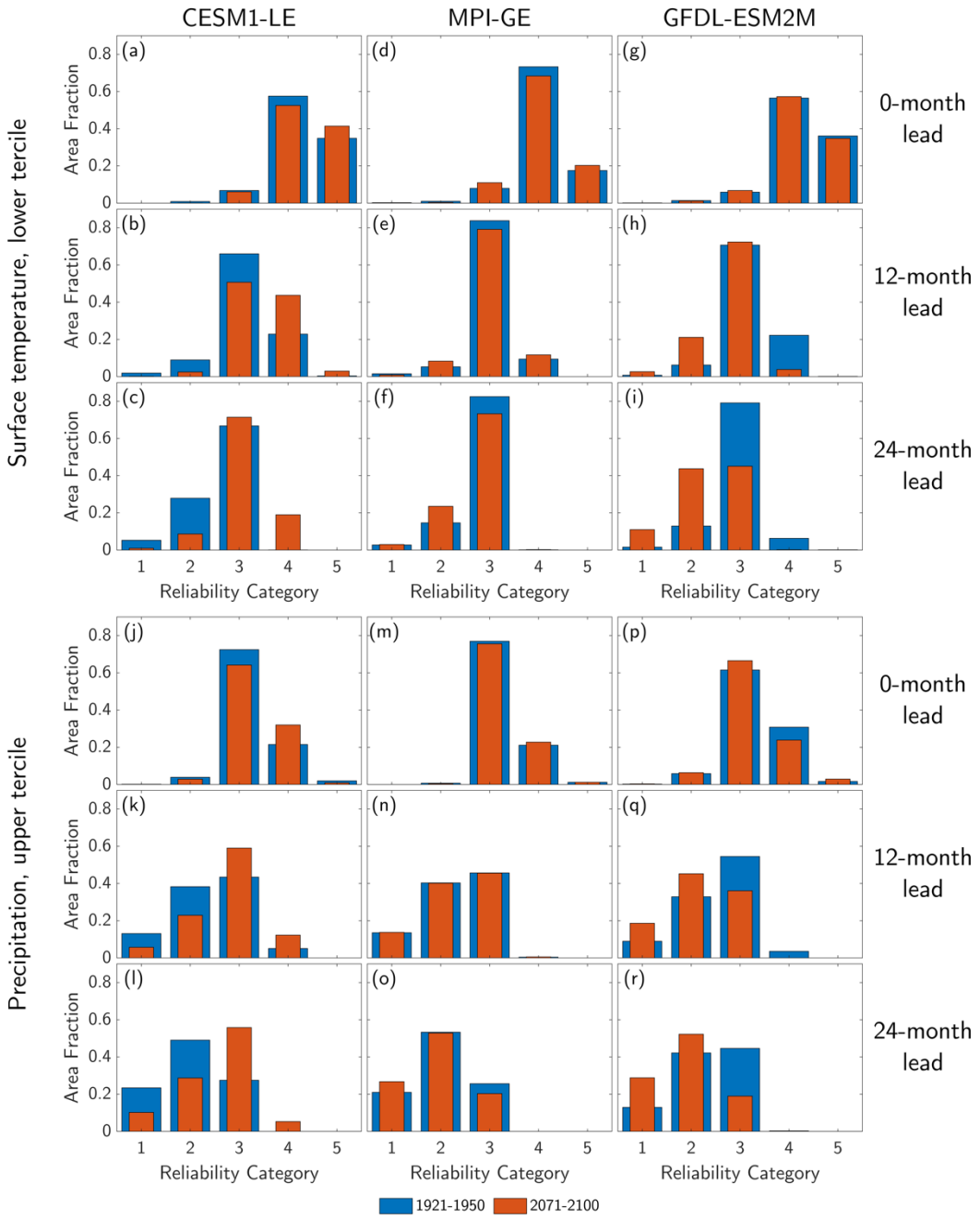

Figure S16 Fraction of global area in each reliability category for (a)-(i) forecasts of lower tercile surface temperature anomalies and (j)-(r) forecasts of upper tercile precipitation anomalies. Values are for 0-, 12-, and 24-month leads in (left column) CESM1-LE, (middle column) MPI-GE, and (right column) GFDL-ESM2M. Reliability categories are calculated across all months in the periods (blue) 1921-1950 and (red) 2071-2100.

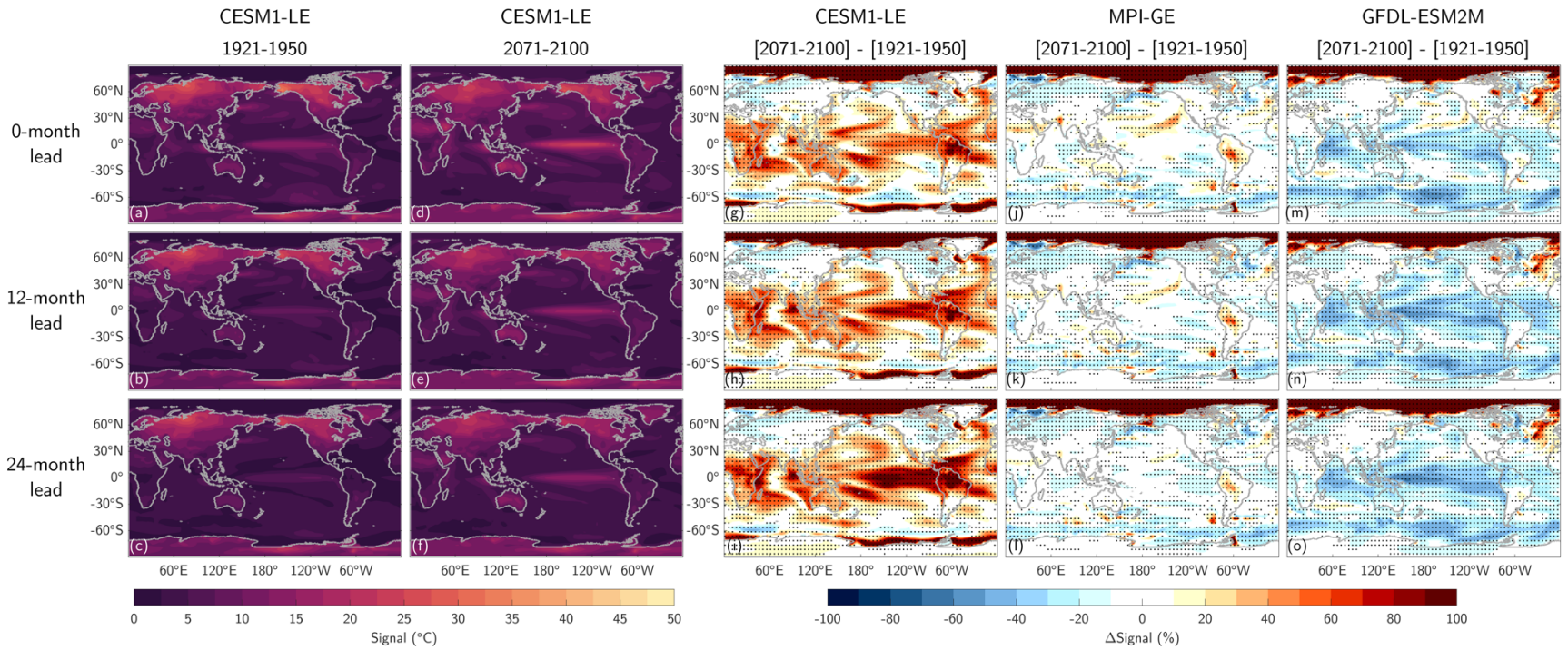

Figure S17 Signal values (˚C) for surface temperature anomaly forecasts (i.e., the numerator of Eq. (1) in main text). (a)-(c) Ensemble mean Signal values of surface temperature forecasts in CESM1-LE calculated across all months in the period 1921-1950. (d)-(f) As in (a)-(c), but for the period 2071-2100. (g)-(o) Percent change in Signal values between past and future periods for (g)-(i) CESM1-LE (j)-(l) MPI-GE (m)-(o) GFDL-ESM2M. Stipples in (g)-(o) indicate where 80% of a respective model's ensemble agrees on the sign of the change.

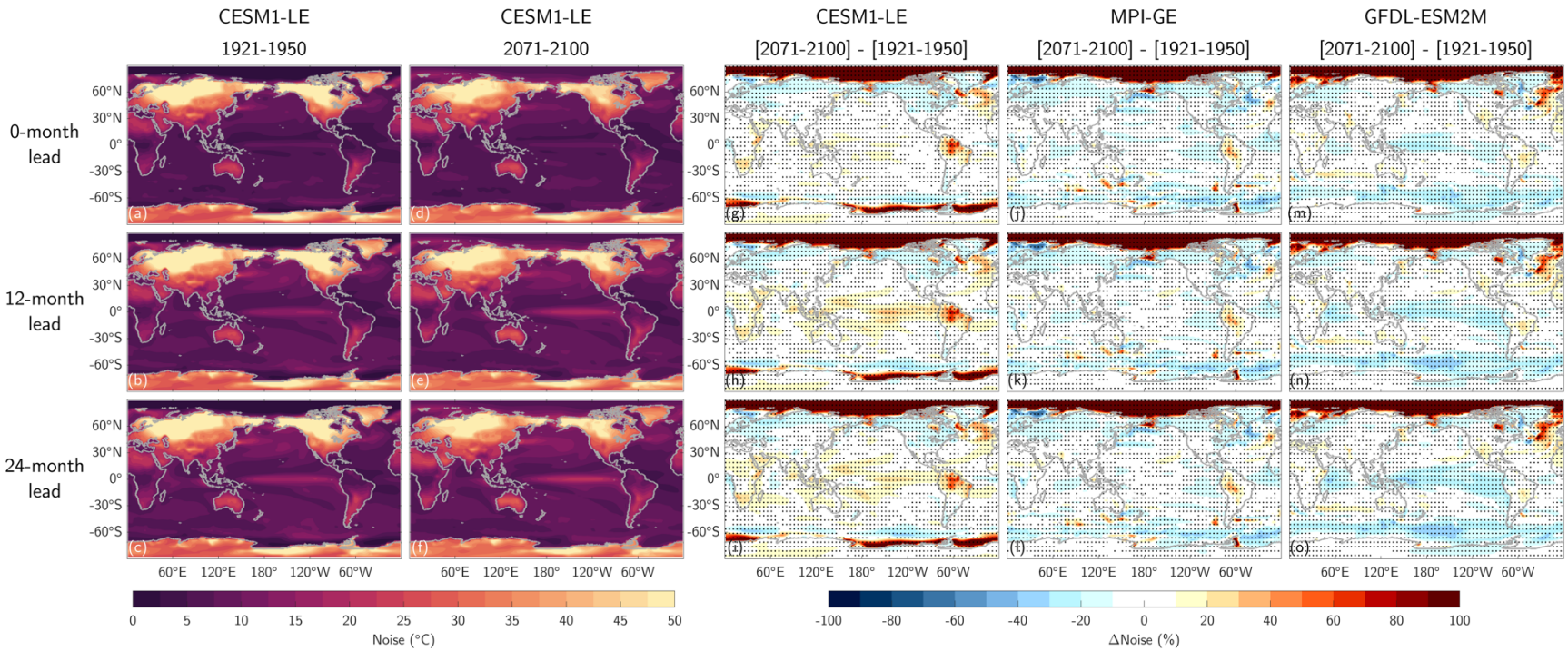

Figure S18 As in Figure S17, but for Noise values (˚C) for surface temperature anomaly forecasts (i.e., the denominator of Eq. (1) in main text).

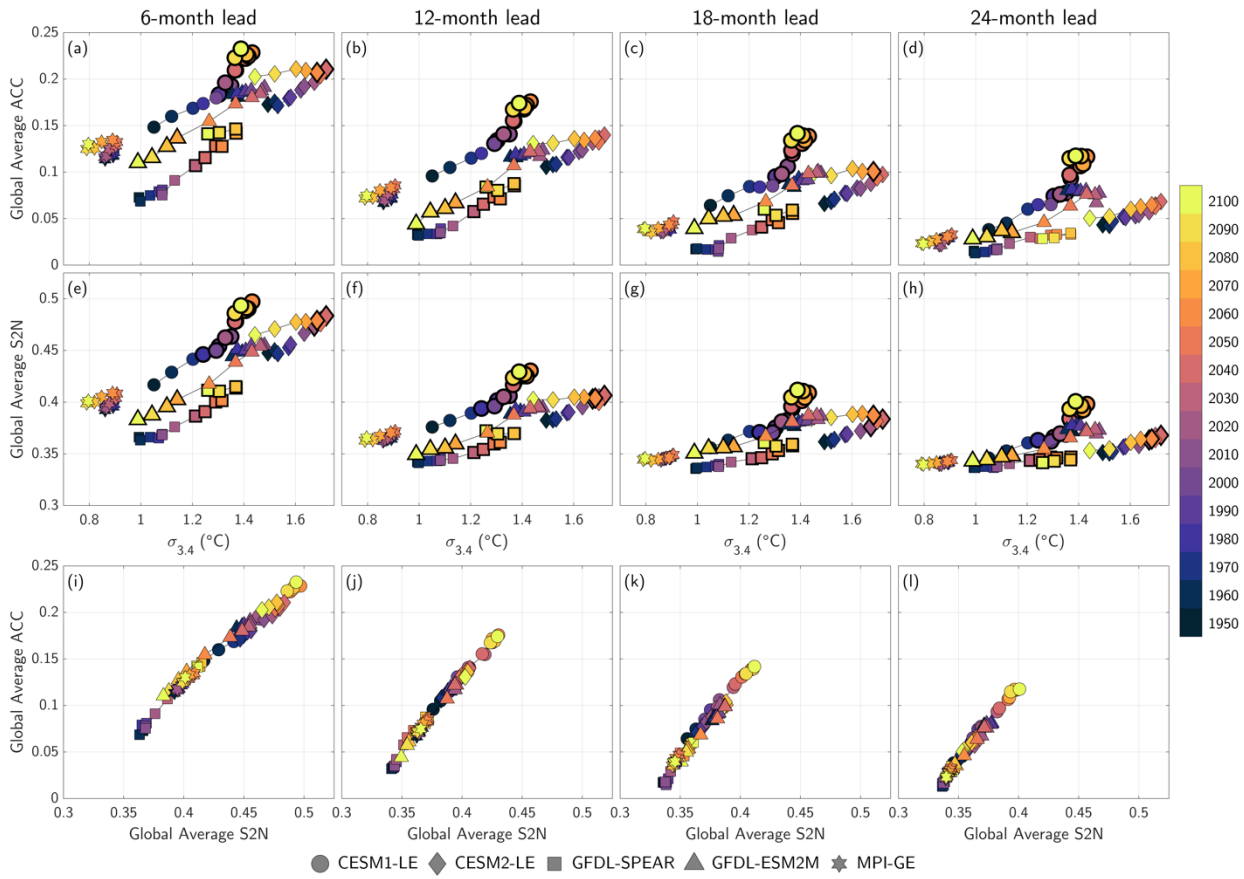

Figure S19 (a)-(d) Global average ensemble mean potential skill at different leads (y-axis) versus December-February averaged Nino3.4 standard deviation (x-axis) in different 30-year periods. (e)-(h) As in (a)-(d), but for global average forecast S2N ratio versus Nino3.4 standard deviation. (i)-(l) As in (a)-(d), but for global average ACC versus global average S2N ratio. All ACC and S2N values are based on ensemble mean SATA forecasts from each model (i.e., different shapes). Shading of each shape indicates the 30-year window over which the forecast skill, S2N ratio or Nino3.4 standard deviation are calculated, with the year indicating the end of the window. For example, the shading for 1950 corresponds to 1921-1950. Markers with bold outlines in (a)-(h) indicate 30-year windows in which 80% of a given model's ensemble agree on the sign of the change (relative to 1921-1950) for both the ACC/S2N and Nino3.4 standard deviation.

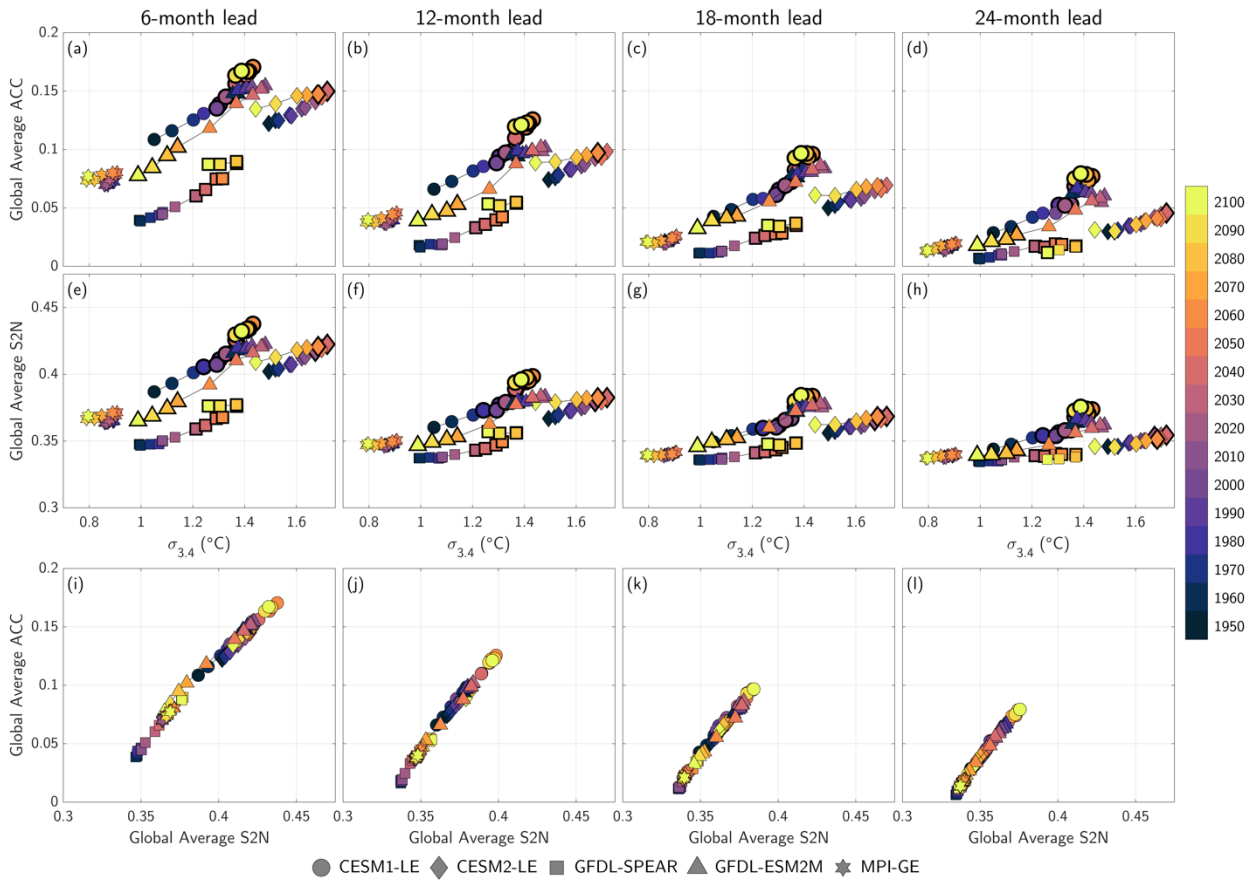

Figure S20 As in Figure S19, but for precipitation anomaly forecasts.